IIETA International Information and Engineering Technology Association
Advancing the World of Information and Engineering

Revue des Composites et des Matériaux Avancés-Journal of Composite and Advanced Materials
Vol. 34, No. 5, October, 2024, pp. 541-547
Journal homepage: http://iieta.org/journals/rcma

# A 3D Model of a Photovoltaic Thermal Panel with the Heat Transfer Fluid Tube Embedded in a Layer of Phase Change Material and Metal Foam

Bernardo Buonomo, Maria Rita Golia, Oronzio Manca, Sergio Nardini*

Dipartimento di Ingegneria, Università degli Studi della Campania "Luigi Vanvitelli", Aversa 81031, Italy

Corresponding Author Email: sergio.nardini@unicampania.it



https://doi.org/10.18280/rcma.340501

**Received:** 17 September 2024
**Revised:** 17 October 2024
**Accepted:** 22 October 2024
**Available online:** 31 October 2024

***Keywords:***
*phase change material (PCM), metal foam (MF), solar energy, photovoltaic*

**ABSTRACT**

Commercial photovoltaic modules typically convert only 5-25% of solar radiation into electricity, wasting excess energy as heat. To improve efficiency, integrating photovoltaic/thermal (PV/T) systems is forward-thinking. These systems generate electricity while using absorbed heat for practical purposes, enhancing efficiency and providing thermal energy for heating. This study analyzes a PV/T module with phase change material (PCM) and metal foam (MF) throughout the typical day of two winter months and two summer months. It investigates how thermal storage affects energy production. Simulations assume heat transfer fluid flow during daylight hours, controlling flow when necessary. Simulations use a heat transfer fluid at 20°C, typical for PV/T systems, with paraffins wax RT25. Performance is simulated for January, June, July, and December in Aversa (IT), with a 30° panel inclination, using data from PVGIS. The study evaluates the reliability of the simulation model and accuracy in representing thermal behavior, using Fluent software. Anticipated outcomes include PV operational hours, electrical and thermal efficiency, and energy output. This research advances efficient PV/T systems, offering insights for future applications.

## 1. INTRODUCTION

Currently, photovoltaic modules can only convert 5 to 25% of incoming solar radiation into electricity, with the rest of the solar energy being converted into heat within the modules, which is often wasted. In contrast, a hybrid PV/T system can capture this excess heat and convert it into usable thermal energy while also generating electricity from solar radiation using PV panels [1]. Mousavi et al. [2] showed that electrical and exergy efficiencies could be optimized by integrating phase change materials and metal foam into the PV-T panel. In their study, they observed that thermal efficiency was lower in configurations lacking the optimized combination of PCM and MF. In the climate of Benha, Egypt, Sharaf et al. [3] investigated the yearly energy and exergy performance of a PV panel in conjunction with aluminium metal foam embedded into pure PCM. They discovered that combining PCM with PV panels improved the efficiency and output of electricity. In order to attain peak performance, careful consideration should go into choosing PCM [4-6]. Moreover, Dayer et al. [7] investigated a 3D model of a PV-T panel incorporating copper metal foam and phase change material (PCM), resulting in reduced PV surface temperature and increased electrical efficiency. In experiments conducted under 1000 W/m$^2$ irradiance and 20°C ambient temperature, the collector exhibited thermal and electrical efficiencies of 65% and 13%, respectively. Sharaf et al. [8] showed that PCM is quite effective at absorbing extra heat from PV panels that would otherwise be wasted. During peak heat periods, the latent heat of PCM is used to keep panel temperatures below 25°C, which improves the overall performance of PV-T system as well as its thermal and electrical efficiency. Alsaqoor et al. [9] investigated the impact of integrating phase change materials into PVT panels and developed a graphic user interface within MATLAB Simulink, using the weather conditions of Amman, Jordan. They found that the maximum electrical power achievable in a PVT system with PCM was 21 kW, compared to 18 kW in a PVT system without PCM. According to Bandaru et al. [10], PVT-PCM systems may store 50% more heat than conventional PVT-water systems, which increases power output and extends the time that thermal energy is available. Nevertheless, poor PCM selection might result in problems like poor heat conductivity and incorrect cycles of charging and discharging, requiring more experimental study to guarantee long-term system integrity and stop leaks. Hossain et al. [11] demonstrated that PCM was used in the development of a hybrid solar PVT system, and its performance was compared with meteorological data from Malaysia. The results show that the use of PCMs improved PV performance (both electrical and thermal). PVT and PVT-PCM collectors were found to have maximum electrical and thermal efficiencies of 14.57% and 15.32%, and 75.29% and 86.19%, respectively. Noxpanco et al. [12] highlighted the necessity of conducting an economic assessment of PV/T systems, stressing the difficulty in acquiring pricing data and arguing in favour of the timely availability of such data to

support engineering and design decisions. Furthermore, they recommended that in order to increase acceptance and efficiency, greater attention should be paid to enhancing the aesthetics of PV/T systems. The purpose of this article is to create a photovoltaic thermal panel 3D module, consisting of a heat transfer tube embedded in a layer of phase change material and metal foam, in order to provide the panel itself with a heat storage capacity that allows it to operate for a greater number of hours compared to a typical photovoltaic thermal panel. Specifically, the layer that acts as insulation in conventional PVT panels has been replaced with a layer of PCM+MF. The analysis was conducted assuming a temperature of the heat transfer fluid at 20°C, and examining the performance of the panel module under environmental conditions of temperature and irradiance typical of January, June, July, and December in Aversa (IT), with an inclination of 30°.

## 2. MODULE DESCRIPTION

It was chosen to analyse the module of a photovoltaic thermal panel composed as follows in Figure 1.

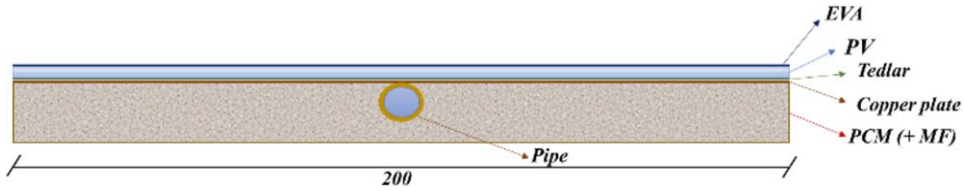


**Figure 1.** Front view of the analyzed PVT module

Table 1 shows the dimensions of the analyzed 3D module, in Figure 2, and in Table 2 data regarding the characteristics of the various materials used in the PVT module are reported.

The RT25 from Rubitherm was chosen as the phase change material, with its characteristics detailed in Table 3. Aluminum foam with PPI20 and 95% porosity was selected as the metal foam.

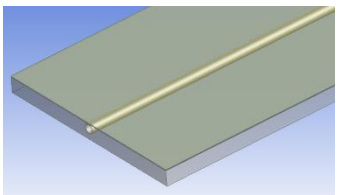

**Figure 2.** 3D module

**Table 1.** Dimensions of the PVT module

| Components | Dimensions [mm] |
|---|---|
| EVA | 1640×200×0.5 (L×W×H) |
| PV unit | 1640×200×0.3 (L×W×H) |
| Tedlar | 1640×200×0.1 (L×W×H) |
| Copper absorber plate | 1640×200×0.4 (L×W×H) |
| Outer diameter of collector pipes | 10 |
| PCM | 1640×200×15 (L×W×H) |

**Table 2.** Properties of components

| **Glass** | | **PV** | |
|---|---|---|---|
| $\alpha$ | 0.01 | $\alpha$ | 0.93 |
| $\rho$ [kg m$^{-3}$] | 2700 | $\rho$ [kg m$^{-3}$] | 2328 |
| $\gamma$ | 0.16 | $\varepsilon$ | 0.90 |
| $\varepsilon$ | 0.90 | $\eta_{ref}$ | 0.126 |
| C [J kg$^{-1}$K$^{-1}$] | 800 | $T_{ref}$ [K] | 294 |
| $\lambda$ [W m$^{-1}$K$^{-1}$] | 1.80 | C [J kg$^{-1}$K$^{-1}$] | 677 |
| s [mm] | 4 | $\lambda$ [W m$^{-1}$K$^{-1}$] | 140 |
| $\tau$ | 0.95 | $\beta$ [K$^{-1}$] | 0.0052 |
| **EVA** | | s [mm] | 0.35 |
| $\lambda$ [W m$^{-1}$K$^{-1}$] | 0.2 | $\tau$ | 0.01 |
| s [mm] | 0.1 | **Tedlar** | |
| **Adhesive** | | $\lambda$ [W m$^{-1}$K$^{-1}$] | 0.35 |
| $\lambda$ [W m$^{-1}$K$^{-1}$] | 0.85 | s [mm] | 0.5 |
| s [mm] | 0.05 | | |

**Table 3.** Properties of RT25

| | |
|---|---|
| **$\rho$ [kg m$^{-3}$]** | 767 |
| **$H_L$ [kJ kg$^{-1}$]** | 232 |
| **C [J kg$^{-1}$ K$^{-1}$]** | 2100 |
| **$\lambda$ [W m$^{-1}$K$^{-1}$]** | 0.185 |
| **$T_s$ [K]** | 298.75 |
| **$T_l$ [K]** | 300.75 |

## 3. ENERGY EQUATIONS AND BOUNDARY CONDITIONS

In this study, several assumptions and simplifications have been incorporated:

-The PV panel components are assumed to exhibit isotropic and homogeneous properties.

-The first layer of the PV unit (EVA) generates incident solar radiation, which is uniform, and it is considered that the transmissivity of the EVA layer is 100%

-There is negligible contact resistance between the various solid components of PVT/PCM systems.

-The analysis does not consider the possible impact of rain on the density of accumulated dust.

-Equations governing the system are expressed in terms of velocity and pressure variables.

-Enthalpy-porosity modeling, following method of Voller and Prakash, is employed for the PCM.

-The influence of gravity is included in this investigation.

-Flow of the heat transfer fluid (HTF), water, through the channel is presumed to be two-dimensional, unsteady, laminar, and incompressible.

-Natural convection within the molten PCM container is considered as two-dimensional, unsteady, laminar, and incompressible.

-The porous medium is treated as saturated, homogeneous, and isotropic.

-Flow within the porous medium is analyzed using the Brinkman–Forchheimer-extended Darcy model.

-Thermo-physical properties are assumed temperature-independent, except for density which varies linearly with temperature (Boussinesq approximation), evaluated at ambient temperature.

-The porous medium analysis is conducted under local thermal equilibrium (LTE) conditions.

### 3.1 Energy equation for PV-layer

The energy equation for PV-layer is:

$$\left(\rho C_p\right)_{PV-layer}\frac{\partial T}{\partial \tau}=\lambda_{PV-layer}\left(\frac{\partial^2 T}{\partial x^2}+\frac{\partial^2 T}{\partial y^2}+\frac{\partial^2 T}{\partial z^2}\right)+Q \tag{1}$$

Q is the internal heat source, $\rho$ is the density, $C$ is the heat capacity (J/(kg·K)) and $\lambda$ is the thermal conductivity.

It has been assumed that heat will be released as a result of the residual solar energy that is absorbed and not transformed into electricity. As a result, this internal heat source causes the temperature of the PV panel to rise. To evaluate Q the Eq. (2) is used:

$$Q=\frac{(1-\eta_{el})G_i A}{V_{PV}} \tag{2}$$

Gi is the absorbed solar radiation, A is the surface of the PV panel and $V_{pv}$ is the volume of the PV cells in the panel.

### 3.2 PCM and metal foam layer

Continuity equation, momentum and energy equations in local thermal equilibrium, were used for PCM and MF.

Continuity equation:

$$\frac{\partial u}{\partial x}+\frac{\partial v}{\partial y}+\frac{\partial w}{\partial z}=0 \tag{3}$$

Momentum equations:

(momentum x)

$$\begin{aligned}&\frac{\rho_{pcm}}{\varepsilon_P}\left(\frac{\partial u}{\partial \tau}+\frac{u}{\varepsilon_P}\frac{\partial u}{\partial x}+\frac{v}{\varepsilon_P}\frac{\partial u}{\partial y}+\frac{w}{\varepsilon_P}\frac{\partial u}{\partial z}\right)=\\&-\frac{\partial p}{\partial x}+\frac{\mu_{pcm}}{\varepsilon_P}\left(\frac{\partial^2 u}{\partial x^2}+\frac{\partial^2 u}{\partial y^2}+\frac{\partial^2 u}{\partial z^2}\right)-\\&\frac{(1-\beta_l)^2}{\left(\beta_l^3-0.001\right)^3}A_{mush}u-\left(\frac{\mu_{pcm}}{K}+\frac{C_F\rho_{pcm}}{\sqrt{K}}|V|\right)u\\&+\rho_{pcm}\gamma\left(T-T_{melt}\right)g\cos(\alpha)\end{aligned} \tag{4}$$

(momentum y)

$$\begin{aligned}&\frac{\rho_{pcm}}{\varepsilon_P}\left(\frac{\partial v}{\partial \tau}+\frac{u}{\varepsilon_P}\frac{\partial v}{\partial x}+\frac{v}{\varepsilon_P}\frac{\partial v}{\partial y}+\frac{w}{\varepsilon_P}\frac{\partial v}{\partial z}\right)=\\&-\frac{\partial p}{\partial y}+\frac{\mu_{pcm}}{\varepsilon_P}\left(\frac{\partial^2 v}{\partial x^2}+\frac{\partial^2 v}{\partial y^2}+\frac{\partial^2 v}{\partial z^2}\right)-\\&\frac{(1-\beta_l)^2}{\left(\beta_l^3-0.001\right)^3}A_{mush}v-\left(\frac{\mu_{pcm}}{K}+\frac{C_F\rho_{pcm}}{\sqrt{K}}|V|\right)v\\&+\rho_{pcm}\gamma\left(T-T_{melt}\right)g\sin(\alpha)\end{aligned} \tag{5}$$

(momentum z)

$$\begin{aligned}&\frac{\rho_{pcm}}{\varepsilon_P}\left(\frac{\partial w}{\partial \tau}+\frac{u}{\varepsilon_P}\frac{\partial w}{\partial x}+\frac{v}{\varepsilon_P}\frac{\partial w}{\partial y}+\frac{w}{\varepsilon_P}\frac{\partial w}{\partial z}\right)=\\&-\frac{\partial p}{\partial z}+\frac{\mu_{pcm}}{\varepsilon_P}\left(\frac{\partial^2 w}{\partial x^2}+\frac{\partial^2 w}{\partial y^2}+\frac{\partial^2 w}{\partial z^2}\right)-\\&\frac{(1-\beta_l)^2}{\left(\beta_l^3-0.001\right)^3}A_{mush}w-\left(\frac{\mu_{pcm}}{K}+\frac{C_F\rho_{pcm}}{\sqrt{K}}|V|\right)w\\&+\rho_{pcm}\gamma\left(T-T_{melt}\right)g\end{aligned} \tag{6}$$

Energy equation in local thermal equilibrium (LTE):

$$\begin{aligned}&(\rho C)_{eff}\frac{\partial v}{\partial \tau}+(\rho C)_{pcm}\left(u\frac{\partial T}{\partial x}+v\frac{\partial T}{\partial y}+w\frac{\partial T}{\partial z}\right)=\\&\lambda_{eff}\left(\frac{\partial^2 T}{\partial x^2}+\frac{\partial^2 T}{\partial y^2}+\frac{\partial^2 T}{\partial z^2}\right)-\varepsilon_P\rho_{pcm}H_L\frac{\partial \beta}{\partial \tau}\end{aligned} \tag{7}$$

In the Eq. (8) $H_L$ represents the latent heat of the PCM, and $t$ is the time.

$$(\rho C)_{eff}=(1-\varepsilon_P)\rho_{mf}C_{mf}+\varepsilon_P\rho_p C_{pcm} \tag{8}$$

$$\lambda_{eff}=(1-\varepsilon_P)\lambda_{mf}+\varepsilon_P\lambda_{pcm} \tag{9}$$

The weighted average is obtained in Eq. (8), and the effective thermal conductivity is calculated in Eq. (9). The density and specific heat of MF and PCM are represented by $\rho_{mf}$, $\rho_{pcm}$, and $C_{mf}$, $C_{pcm}$. The metal foam and PCM thermal conductivities are denoted by $\lambda_{mf}$ and $\lambda_p$. P stands for porosity, K for permeability [$m^2$] (viscous drag or Darcy drag), and $C_F$ for Forcheimer coefficient (inertial drag) in the case of the metal foam. Regarding the phase change material, $H_L$ stands for specific heat latent [J/kg], $A_{mush}$ is an empirical constant that fluctuates between $10^5$ and $10^8$, and $\beta_l$ is the liquid fraction.

## 4. PERFORMANCE EVALUATION

The photovoltaic thermal module efficiency was calculated applying the following formulas. The electrical efficiency ($\eta_{el}$) of the PV cells is described by Nouira and Sammouda [13]:

$$\eta_{el}=\eta_{ref}\left(1-\beta_{ref}\left(T_{PV}-T_{ref}\right)\right) \tag{10}$$

where, $\eta_{ref}$ , $\beta_{ref}$ and $T_{ref}$ are panel parameters, listed in Table 1. The formula to determine the instantaneous electrical power of the module is Eq. (11):

$$P_{out}=\eta_{el}AG_i \tag{11}$$

The energy produced by the panel was obtained by multiplying the annual average of the power by the total number of hours the panel is operated. PVGIS data was consulted for data concerning solar radiation and ambient temperature. In addition, the change in Tsky was calculated as follows by Swinbank [14]:

$$T_{sky} = 0.0552 \cdot T_{amb}^{1.5} \quad (12)$$

Both the thermal energy generated by the water moving through the channel and the thermal energy brought on by the presence of PCM were measured.

In order to accomplish this, the heat transfer rate of channel is:

$$\dot{E}_f = \dot{m}_f C_f (T_{f,out} - T_{f,in}) \quad (13)$$

where $\dot{m}_f$ is the mass flow rate, $C_f$ is the specific heat and $T_{f,out}$, $T_{f,in}$ are the temperature of the heat transfer fluid on inlet and outlet. In our scenario, the temperature at the inlet section remains constant, assuming control over the fluid temperature within the system.

Integrating over time yields the total thermal energy generated by the channel.

$$W_f = \int E_f(t)dt \quad (14)$$

The process was repeated for the thermal energy produced by the PCM. Beginning with the enthalpy of the PCM, its variation over time was determined, leading to the calculation of the heat transfer rate of the PCM as:

$$\dot{E}_{PCM} = \frac{dH}{dt} \quad (15)$$

Next, integrating over time yielded the accumulated thermal energy stored:

$$W_{PCM} = \int E_{PCM}(t)dt \quad (16)$$

Regarding the thermal aspect, when comparing the thermal efficiency of a PVT module without PCM to one with PCM, it is observed that the module without PCM exhibits higher thermal efficiency [15]. Eq. (17) exclusively accounts for the thermal characteristics of the fluid [16]:

$$\eta_{th,f} = \frac{\dot{E}_f}{\dot{E}_{sun}} \quad (17)$$

Where in Eq. (17), the numerator represents the thermal power of the channel, and Gi represents the solar radiation incident on the PV/T system [17].

$$\dot{E}_{sun} = \tau_g \alpha_{PV} G_i A_{PV} \quad (18)$$

In our case, with the tube embedded in a layer of PCM, the thermal energy generated by the panel can be expressed as:

$$\dot{E}_{th} = \dot{E}_f + \dot{E}_{PCM} \quad (19)$$

And the total thermal efficiency is:

$$\eta_{th} = \frac{\dot{E}_f + \dot{E}_{PCM}}{\dot{E}_{sun}} \quad (20)$$

## 5. MODEL VALIDATION

The model was validated based on the 3D model by Kazemian et al. [18], which had previously been validated by them through comparison of the numerical results obtained with the numerical work of Su et al. [19] and the experimental work of Browne et al. [20]. The properties of the various components used in the simulation are listed in Table 4.

**Table 4.** Characteristics validation components

| Components | ρ [kg m$^{-3}$] | C [J kg$^{-1}$ K$^{-1}$] | λ [W m$^{-1}$ K$^{-1}$] |
|---|---|---|---|
| EVA | 960 | 2090 | 0.35 |
| PV | 2330 | 700 | 1.48 |
| Tedlar | 1220 | 1250 | 0.20 |
| Absorber plate | 8960 | 385 | 401 |

In the numerical simulation, the calculation time for the unsteady model is set at two hours, during which the average electrical and thermal efficiencies are computed. The same boundary conditions were recreated and used the same numerical methods. The PCM used has the characteristics listed in Table 5 [15].

**Table 5.** Properties of the PCM used in validation [15]

| | |
|---|---|
| **ρ [kg m$^{-3}$]** | 800 |
| **$H_L$ [kJ kg$^{-1}$]** | 170 |
| **C [J kg$^{-1}$ K$^{-1}$]** | 2300 |
| **λ [W m$^{-1}$K$^{-1}$]** | 0.25 |
| **$T_s$ [K]** | 324.15 |
| **$T_l$ [K]** | 330.15 |

The temperature of the outdoor environment is set at 30°C for 2 hours of simulation. In Figure 3 the temperature of the heat transfer fluid (water) is set at 30°C, and the fluid velocity in the single channel is 0.0281 m/s. It was compared the surface temperature of the photovoltaic panel in the base case with a $T_0$ = 30°C and solar radiation of 800 W/m$^2$.

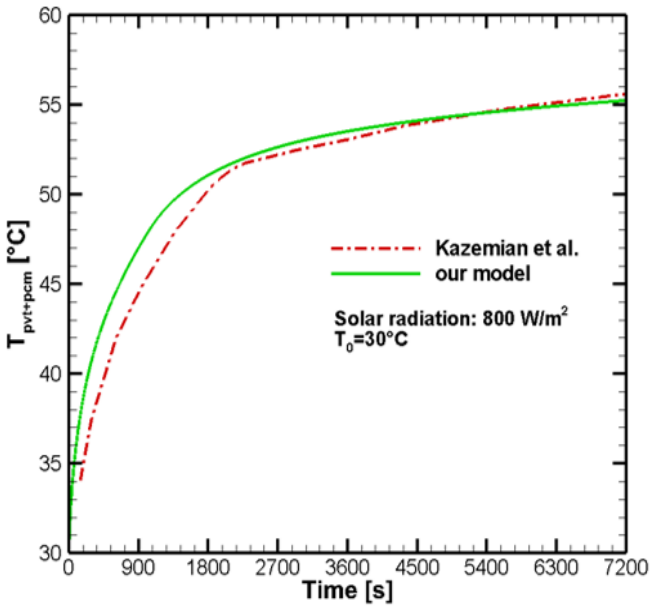


**Figure 3.** Comparison between PVT+PCM surface temperature of the Kazemian et al. [15] model and our model

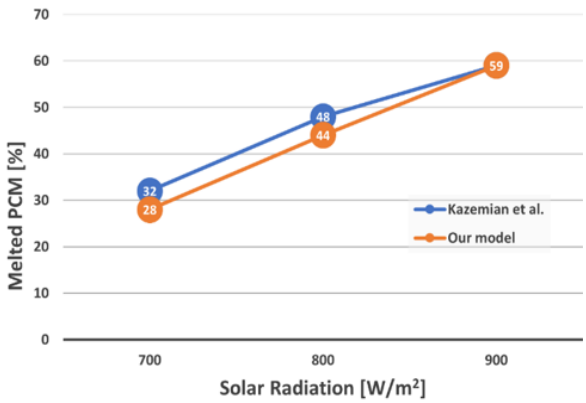


**Figure 4.** Comperison, in terms of the melted PCM percentage vs solar radiation, between present model and Kazemian et al. [18] model

Then, Figure 4 shows the comparison of the melting rate of the phase change material as the solar radiation on the panel changes. The obtained results show good agreement between the model of Kazemian et al. [18] and our model.

## 6. RESULTS

### 6.1 Electrical energy

The average day of January, June, July, and December was used for the simulations, and the results were presented in terms of power production, electrical efficiency, and panel operating hours of the photovoltaic panel.

Only the hours with solar irradiation—which correspond to the real working hours of photovoltaic panel—were taken into consideration from the electrical point of view of panel module. The graphs, in Figure 5, demonstrate that the PV module with PCM+MF state has a higher electrical efficiency than the case without the storage layer. This is especially noticeable during winter months, as the presence of PCM+MF allows the photovoltaic panel to maintain a temperature closer to the optimal working temperature, as it absorbs heat. There is a shift in tendency at the end of the day when solar radiation becomes less intense. This is because, in the last hour of the day, the panel cools down more quickly and exhibits higher electrical efficiency due to the module without PCM heating up and cooling down more quickly. On the other hand, the efficiency of the PCM+MF panel is slightly lower than that of the PCM-free panel because the heat that accumulates during the day needs to be gradually dissipated.

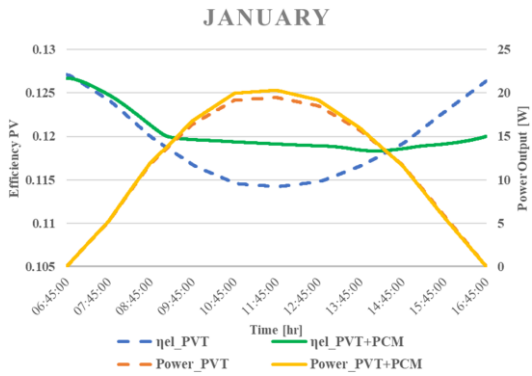


(a) Typical day of January

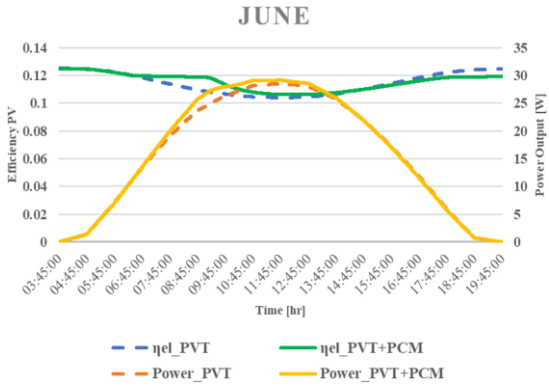


(b) Typical day of June

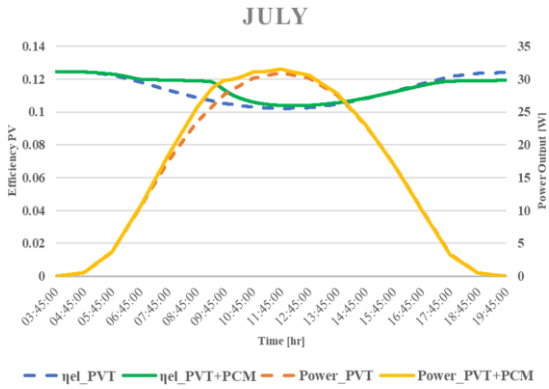


(c) Typical day of July

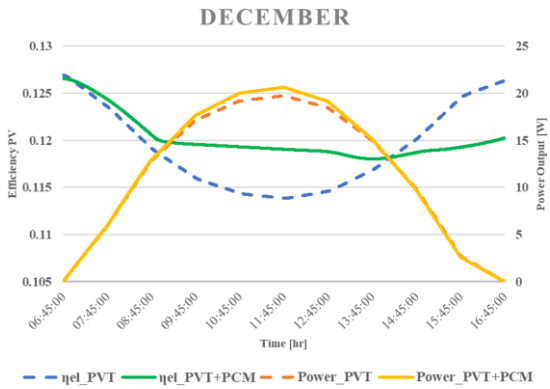


(d) Typical day of December

**Figure 5.** Time evolution of efficiency and power output

In general, compared to panels without an accumulation layer, solar panels with a PCM+MF layer have more stable efficiency over the winter. Production of electricity is impacted by efficiency, however as the results demonstrate, there is not much difference in efficiency and noticeable variations are only seen at periods of maximum solar radiation. In fact, a considerable variation in efficiency between panels with and without PCM has little effect on power output during the early and late hours of the day when solar radiation is low.

The data collected indicates that there has been a 2% increase in electricity generation when comparing a solar module with and without an accumulation layer.

### 6.2 Thermal energy

From the perspective of thermal energy efficiency, the

system does not show significant improvements; however, when considering the number of operating hours, in Table 6, there is an extension of the operating period. This can be observed both in summer and winter months but is more pronounced in winter months. In fact, the percentage increase in the operating period is approximately 40% and 42% for January and December, and 29% and 28% for June and July. Therefore, the presence of the PCM+MF layer extends the operating hours of the module under consideration. The operating hours were calculated by considering the outlet temperature to be higher than the inlet temperature.

**Table 6.** Operating hours

| | No PCM | PCM | % |
|---|---|---|---|
| January | 6.1 h | 10.1 h | 40 |
| June | 12.2 h | 17.1 h | 29 |
| July | 12.6 h | 17.4 h | 28 |
| December | 5.9 h | 10.1 h | 42 |

## 7. CONCLUSIONS

Based on the simulations and analysis conducted for different months throughout the year, several conclusions can be concluded regarding the performance of the PV panel with and without a PCM and MF layer. The PV module with the PCM+MF layer demonstrates higher electrical efficiency compared to the module without the storage layer, especially noticeable during winter months. The presence of the PCM+MF layer contributes to a more consistent efficiency throughout the day, particularly in winter, by absorbing excess heat and extending the effective operating period of the PV panel. This enhancement is attributed to the PCM+MF layer enabling the PV panel to maintain a temperature closer to the optimal operating range. Additionally, there is a notable extension in the operating hours of the system due to the effective heat storage and release capabilities of PCM+MF, with the operating period extension being more pronounced during winter months. In summary, the incorporation of a PCM+MF layer into the PV module results in improved electrical efficiency, maintained performance under varying solar conditions, and significantly extended hours of operation. These results highlight the potential benefits of using phase change materials and metal foams to improve the performance and effectiveness of photovoltaic systems, especially to optimize energy production and utilization in different seasons.

## ACKNOWLEDGMENT

This work was supported by the Italian Government MUR Grant No. P2022NYPHL – PRIN 2022 PNRR "VISIONS: eVolutIonary deSign of InnOvative heat traNsfer deviceS" – Funded by European Union – Next Generation EU. This work was also supported by PON R&I 2014-2020 - Azione IV.5 GREEN-MRG.

## REFERENCES

[1] Preet, S. (2021). A review on the outlook of thermal management of photovoltaic panel using phase change material. Energy and Climate Change, 2: 100033. https://doi.org/10.1016/j.egycc.2021.100033

[2] Mousavi, S., Kasaeian, A., Shafii, M.B., Jahangir, M.H. (2018). Numerical investigation of the effects of a copper foam filled with phase change materials in a water-cooled photovoltaic/thermal system. Energy Conversion and Management, 163: 187-195. https://doi.org/10.1016/j.enconman.2018.02.039

[3] Sharaf, M., Yousef, M.S., Huzayyin, A.S. (2022). Year-round energy and exergy performance investigation of a photovoltaic panel coupled with metal foam/phase change material composite. Renewable Energy, 189: 777-789. https://doi.org/10.1016/j.renene.2022.03.071

[4] Buonomo, B., Golia, M.R., Manca, O., Nardini, S. (2024). A review on thermal energy storage with phase change materials enhanced by metal foams. Thermal Science and Engineering Progress, 54: 102732. https://doi.org/10.1016/j.tsep.2024.102732

[5] Elmeriah, A., Nehari, D., Mohamed, A., Remlaoui, A. (2018). Natural convection mechanism evaluation inside a shell and tube thermal energy storage (TES) devise inclination. Revue des Composites et des Materiaux Avances, 28(2): 257-276. https://doi.org/10.3166/RCMA.28.257-276

[6] Tao, Y.B., Liu, Y.K., He, Y.L. (2019). Effect of carbon nanomaterial on latent heat storage performance of carbonate salts in horizontal concentric tube. Energy, 185: 994-1004. https://doi.org/10.1016/j.energy.2019.07.106

[7] Dayer, M., Sopian, K., Ibrahim, A., Al-Aasam, A.B., Abdulsahib, B., Rahmanian, S., Abd Hamid, A.S. (2023). Performance of combined PCM/metal foam-based photovoltaic thermal (PVT) collector. International Journal of Renewable Energy Research (IJRER), 13(2): 551-559. https://doi.org/10.20508/ijrer.v13i2.13881.g8723

[8] Sharaf, M., Yousef, M.S., Huzayyin, A.S. (2022). Review of cooling techniques used to enhance the efficiency of photovoltaic power systems. Environmental Science and Pollution Research, 29(18): 26131-26159. https://doi.org/10.1007/s11356-022-18719-9

[9] Alsaqoor, S., Alqatamin, A., Alahmer, A., Nan, Z., Al-Husban, Y., Jouhara, H. (2023). The impact of phase change material on photovoltaic thermal (PVT) systems: A numerical study. International Journal of Thermofluids, 18: 100365. https://doi.org/10.1016/j.ijft.2023.100365

[10] Bandaru, S.H., Becerra, V., Khanna, S., Radulovic, J., Hutchinson, D., Khusainov, R. (2021). A review of photovoltaic thermal (PVT) technology for residential applications: Performance indicators, progress, and opportunities. Energies, 14(13): 3853. https://doi.org/10.3390/en14133853

[11] Hossain, M.S., Kumar, L., Arshad, A., Selvaraj, J., Pandey, A.K., Rahim, N.A. (2023). A comparative investigation on solar PVT-and PVT-PCM-based collector constancy performance. Energies, 16(5): 2224. https://doi.org/10.3390/en16052224

[12] Noxpanco, M.G., Wilkins, J., Riffat, S. (2020). A review of the recent development of photovoltaic/thermal (Pv/t) systems and their applications. Future Cities and Environment, 6(1): 9. https://doi.org/10.5334/fce.97

[13] Nouira, M., Sammouda, H. (2018). Numerical study of an inclined photovoltaic system coupled with phase

change material under various operating conditions. Applied Thermal Engineering, 141: 958-975. https://doi.org/10.1016/j.applthermaleng.2018.06.039
[14] Swinbank, W.C. (1963). Long-wave radiation from clear skies. Quarterly Journal of the Royal Meteorological Society, 89(381): 339-348. https://doi.org/10.1002/qj.49708938105
[15] Preet, S., Bhushan, B., Mahajan, T. (2017). Experimental investigation of water based photovoltaic/thermal (PV/T) system with and without phase change material (PCM). Solar Energy, 155: 1104-1120. https://doi.org/10.1016/j.solener.2017.07.040
[16] Duffie, J.A., Beckman, W.A., Blair, N. (2020). Solar Engineering of Thermal Processes, Photovoltaics and Wind. John Wiley & Sons. https://doi.org/10.1002/9781118671603
[17] Abbas, S., Zhou, J., Hassan, A., Yuan, Y., Yousuf, S., Sun, Y., Zeng, C. (2023). Economic evaluation and annual performance analysis of a novel series-coupled PV/T and solar TC with solar direct expansion heat pump system: An experimental and numerical study. Renewable Energy, 204: 400-420. https://doi.org/10.1016/j.renene.2023.01.032
[18] Kazemian, A., Salari, A., Hakkaki-Fard, A., Ma, T. (2019). Numerical investigation and parametric analysis of a photovoltaic thermal system integrated with phase change material. Applied Energy, 238: 734-746. https://doi.org/10.1016/j.apenergy.2019.01.103
[19] Su, D., Jia, Y., Lin, Y., Fang, G. (2017). Maximizing the energy output of a photovoltaic–thermal solar collector incorporating phase change materials. Energy and Buildings, 153: 382-391. https://doi.org/10.1016/j.enbuild.2017.08.027
[20] Browne, M.C., Norton, B., McCormack, S.J. (2016). Heat retention of a photovoltaic/thermal collector with PCM. Solar Energy, 133: 533-548. https://doi.org/10.1016/j.solener.2016.04.024

## NOMENCLATURE

| | |
|---|---|
| $C$ | specific heat, J kg$^{-1}$ K$^{-1}$ |
| $g$ | gravitational acceleration, m s$^{-2}$ |
| $H_L$ | heat of fusion, kJ kg$^{-1}$ |
| $s$ | thickness, mm |
| $T$ | temperature, K |
| $T_l$ | melting temperature, K |
| $T_s$ | freezing temperature, K |

### Greek symbols

| | |
|---|---|
| $\alpha$ | absorptivity |
| $\beta$ | thermal expansion coefficient, K$^{-1}$ |
| $\beta_l$ | liquid fraction |
| $\gamma$ | diffuse reflection coefficient |
| $\varepsilon$ | emissivity |
| $\varepsilon_p$ | porosity |
| $\eta$ | efficiency |
| $\lambda$ | thermal conductivity, Wm$^{-1}$K$^{-1}$ |
| $\mu$ | dynamic viscosity, kg m$^{-1}$s$^{-1}$ |
| $\rho$ | density, kg m$^{-3}$ |
| $\tau$ | transmissivity |

### Subscripts

| | |
|---|---|
| *el* | electrical |
| *f* | heat transfer fluid |
| *g* | glass |
| *mf* | metal foam |
| *pcm* | phase change material |
| *th* | thermal |